Stress–Strain Isotherms for Elastomers Cross-Linked in Solution. 2. Interpretation in Terms of the Constrained-Chain Model

B. Erman*

School of Engineering and Polymer Research Center, Bogazici University, Bebek 80815, Turkey

J. E. Mark

Department of Chemistry and the Polymer Research Center, University of Cincinnati, Cincinnati, Ohio 45221-0172

Received August 5, 1991; Revised Manuscript Received December 18, 1991

ABSTRACT: The previous interpretation of stress–strain data for poly(dimethylsiloxane) networks cross-linked in solution (Erman, B.; Mark, J. E. *Macromolecules* 1987, *20*, 2892) showed that the κ parameter of the constrained-junction model depended on the volume fraction v_{2c} of the polymer present during cross-linking according to the relation $\kappa = A(2C_1)^{-1/2}v_{2c}^{4/3+m}$, where $2C_1$ is the Mooney–Rivlin constant directly related to the cross-link density. Interpretation of the data according to the constrained-junction model showed that A could be taken to be equal to 2 and that m should vary between $^2/_3$ and $^8/_9$ to give the best fit, whereas theoretical arguments based on a molecular picture of the network require that m should be zero. The same data are now analyzed according to the constrained-chain model, which is more realistic because it spreads out the effects of the constraints along the entire chain contours making up the network. The new analysis indicates that the experimental results may be satisfactorily described by taking $A = 1.29$ and $m = 0.385$. If additional experimental results on other polymeric networks show these values to be universal, this would give important insight into elastomeric properties and provide considerable predictive capabilities.

Introduction

The simplest theories of rubberlike elasticity assume that the elastic free energy of a deformed network is the sum of the elastic free energies of the individual chains and that intermolecular contributions are negligible.[1] The chains according to these theories are phantomlike; i.e., they do not interact with each other along their contours, and their interaction with the rest of the network is only through the two junctions at their extremities. In the affine network model, the junctions of the phantomlike chains are rigidly embedded in the surrounding matrix and deform affinely (linearly) with macroscopic deformation. In the phantom model, the ends may fluctuate in space. In networks with typical junction functionalities, the magnitudes of these fluctuations are indeed large and equate to a significant fraction of the chains' dimensions.

The phantomlike idealization of the network chains may be closely approached if the experiments are performed in the highly swollen state, because in this state the chains are widely separated from one another and their only contact with the rest of the network is through their junctions. The phantom network therefore forms a plausible model for describing the behavior of such highly swollen networks. As the degree of swelling is decreased, the chains start to experience the effects of one another. In uniaxial tension experiments, the onset of intermolecular effects upon removal of the solvent is evidenced by a dependence of the shear modulus on deformation. As the solvent is progressively removed, the ratio $2C_2/2C_1$ of the Mooney constants increases. The undiluted network represents the limiting case where intermolecular interactions are at a maximum.

Introduction of intermolecular interactions in a systematic way into a molecular theory of rubberlike elasticity has been the subject of study over the past 20 years. According to the model proposed by Langley, Ferry, and Graessley and later improved by Edwards and co-workers,[2] intermolecular contributions to the modulus are accounted for by a determinable number of trapped entanglements. These models may in general be referred to as the slip-link type, where the contributions to the modulus by the trapped entanglements are mathematically treated as slip-links that may move along the contour of the chains. According to Flory, such contributions are not gauged by their numbers but by their effect of constraining the fluctuations of the network chains.[3] Such constraining effects are most pronounced at the junctions of the chains. Thus, as a first-order approximation, interactions along the chain contours may be ignored and all intermolecular effects may be concentrated at the junctions. These ideas, first suggested by Ronca and Allegra,[4] have resulted in a workable model of real networks[3] which has later been referred to as the constrained-junction model. The simplifying assumption of applying the constraints at the junctions has recently been removed in a model[5] where intermolecular effects are assumed to hinder the fluctuations of the radii of gyration of the network chains. This model is essentially an extension of the constrained-junction model and may be referred to as the constrained-chain model.

The molecular models referred to above have the common feature that they acknowledge the copious interpenetration or entanglement of the chains in the bulk state as the source of deviation from phantom behavior. Networks prepared in the highly diluted state may therefore be taken as the reference state where the degree of interpenetration is minimized. Networks having varying degrees of interpenetration, formed in different states of swelling, may then be used in the interpretation of the theoretical models.

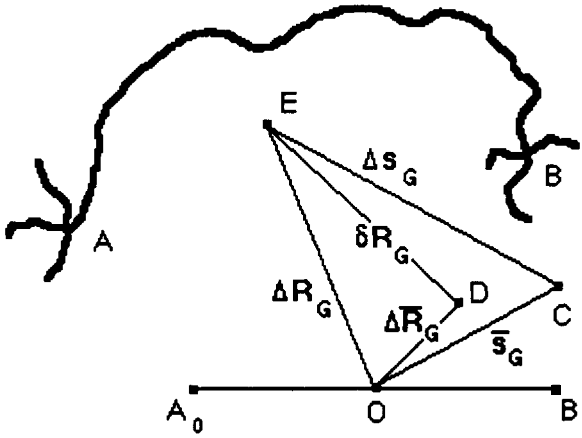

Figure 1. Illustrative instantaneous spatial configuration of a network chain terminated by junctions A and B, the locations of its center of mass, and its fluctuations. See text for details.

In a recent study,[6] we have interpreted the moduli of poly(dimethylsiloxane) (PDMS) networks cross-linked in different states of dilution by using the constrained-junction model. The κ parameter of this model is predicted to scale with the $^4/_3$ power of the degree of swelling, v_{2c}, during network formation. For satisfactory agreement between theory and experiment, however, κ had to scale according to the relationship $\kappa \sim v_{2c}{}^{4/3+m}$, with m varying between $^2/_3$ and $^8/_9$. In the present study, we compare predictions of the constrained-chain model with results of these experiments and conclude that an $m = 0.385$ dependence is obeyed.

In the first section below, we summarize the features of the constrained-chain model and derive the theoretical $^4/_3$ power dependence of κ on v_{2c}. In the next section, we interpret results of the experiments in terms of the constrained-chain model, followed by a discussion of the effect of constraints in networks in general.

Theory

Elastic Free Energy of the Constrained-Chain Model.[5] In Figure 1, an instantaneous configuration of a network chain is shown by the line AB. The straight line A_0B_0 denotes the time-averaged locus of the chain in the phantom network. The midpoint O of A_0B_0 is the location of the time-averaged center of the chain in the phanton network, where the term center is used here to denote the geometric center of the chain. It may also loosely be referred to as the mass center. The difference is inconsequential in the present treatment of network elasticity. In the real network the time-averaged center of the chain will be at some other location due to the effect of entanglements. Point C denotes the time-averaged location $\mathbf{s}_G$ of entanglements that operate on the chain AB. Under the combined effect of the phantom network and the entanglements, the average position $\Delta\bar{\mathbf{R}}_G$ of the center of the chain relative to point O will be located at point D. The quantity $\Delta\mathbf{R}_G$ is the instantaneous fluctuation of the chain center from the phantom network center O. Under the combined effects of the phantom network and constraints, the instantaneous position $\delta\mathbf{R}_G$ of the center of the chain relative to point D is denoted by point E. The mean-squared fluctuation of the center of the chain about the phantom center O in the absence of constraints is given according to theory as

$$\langle(\Delta X_G)^2\rangle_0 = \langle x^2\rangle_0/4(1-2/\phi) \qquad (1)$$

where ΔX_G and x denote the x-components of $\Delta\mathbf{R}_G$ and the chain end-to-end vector, respectively. The fluctuation of the instantaneous chain center $\Delta\mathbf{s}_G$ from the center of the constraints determines the degree of the constraints. The important quantity for determining the departure of the real network behavior from that of the phantom network is the κ_G parameter defined as

$$\kappa_G = \langle(\Delta X_G)^2\rangle_0/\langle(\Delta x_G)^2\rangle_0 \qquad (2)$$

where $\langle(\Delta x_G)^2\rangle_0$ is the x-component of $\Delta\mathbf{s}_G$. In the limit of negligible entanglements, this ratio equates to zero. In the other limit, where the entanglements are extremely strong, it equates to infinity.

The state of deformation for simple tension is given as

$$\lambda_x \equiv \lambda = (v_{2C}/v_2)^{1/3}\alpha$$

$$\lambda_y = \lambda_z = (v_{2C}/v_2)^{1/3}\alpha^{-1/2} \qquad (3)$$

where the extension λ, defined as the ratio of the final length to that in the reference state, is applied along the x-axis. The reference state may be identified with that existing during the formation of the network. The quantity α is a measure of the distortion defined as the ratio of the final length to the undistorted but swollen length, and v_2 is the volume fraction of the polymer in the network during the stress–strain experiment.

The elastic free energy of the network in simple tension is obtained in terms of κ_G and λ as

$$\Delta A_{el} = \frac{1}{2}\xi kT\sum[\lambda_t{}^2 + B_t + D_t - \ln(1 + B_t) - \ln(1 + D_t)] \qquad (4)$$

where the summation over t is carried out for x, y, and z. The factor ξ is the cycle rank of the network and

$$B_x = h(\lambda_x)^2\,(\lambda_x{}^2 - 1)/[\lambda_x{}^2 + h(\lambda_x)]^2$$

$$D_x = \lambda_x{}^2 B_x/h(\lambda_x) \qquad (5)$$

$$h(\lambda_x) = \kappa_G[1 + (\lambda_x{}^2 - 1)\Phi]^{-1}$$

with similar expressions for the y and z components. The parameter Φ is given by theory as

$$\Phi = (1 - 2/\phi)^2(1/3 + 2/3n) \qquad (6)$$

Here, n is the number of freely-jointed segments in a network chain. Within a first-order approximation, the ratio $2/3n$ may be equated to zero.

Equation of State. The force f acting on the sample in the direction of extension is obtained from the thermodynamic relation[7]

$$f = 2L^{-1}\lambda^2(\partial\Delta A_{el}/\partial\lambda^2)_{T,V} \qquad (7)$$

where the subscripts T and V indicate that differentiation is performed at constant temperature and volume. Differentiating eq 4 with respect to λ^2 and substituting in eq 7 leads to

$$f = (\xi kT/L_0)(v_{2c}/v_2)^{1/3}\{\alpha - \alpha^{-2} + (\nu/\xi)[\alpha K(\lambda_x{}^2) - \alpha^{-2}K(\lambda_y{}^2)]\} \qquad (8)$$

Here, ν is the number of chains in the network, L_0 is the length in the reference state, and the function K is defined as

$$K(\lambda^2) = \frac{B\dot{B}}{(1 + B)} + \frac{D\dot{D}}{(1 + D)} \qquad (9)$$

with

$$B = h(\lambda)^2\,(\lambda^2 - 1)/[\lambda^2 + h(\lambda)]^2$$

$$D = \lambda^2 B/h(\lambda) \qquad (10)$$

$$\dot{B} \equiv \frac{\partial B}{\partial \lambda^2} = B\left\{(\lambda^2 - 1)^{-1} - 2[\lambda^2 + h(\lambda)]^{-1} - 2\,\frac{h(\lambda)\,\lambda^2\Phi}{\kappa_G[\lambda^2 + h(\lambda)]}\right\}$$

$$\dot{D} \equiv \frac{\partial D}{\partial \lambda^2} = B\left[h(\lambda)^{-1} + \frac{\lambda^2\Phi}{\kappa_G}\right] + \frac{\lambda^2\dot{B}}{h(\lambda)}$$

The reduced force for the case of uniaxial tension is defined by the expression

$$[f^*] \equiv \frac{f v_2^{1/3}}{A_d(\alpha - \alpha^{-2})} \qquad (11)$$

where A_d is the cross-sectional area of the dry undeformed network. Substituting eqs 8 and 9 into eq 10 leads to the expression

$$[f^*] = [f^*]_{ph}\{1 + (\nu/\xi)[\alpha K(\lambda_x^2) - \alpha^{-2}K(\lambda_y^2)]/(\alpha - \alpha^{-2})\} \qquad (12)$$

Here, $[f^*]_{ph}$ denotes the reduced force for the phantom network defined as

$$[f^*]_{ph} = (\xi kT/V_d)v_{2c}^{2/3} = 2C_1 \qquad (13)$$

with the parameter $2C_1$ denoting the Mooney–Rivlin constant.

Relationship of the κ Parameter to Molecular Parameters and to v_{2c}. Following the arguments of the constrained-junction model,[8] we suggest that the k parameter is proportional to the number of chains sharing the volume occupied by one chain. One can therefore write the equality

$$\kappa = I\langle r^2\rangle_0^{3/2}(\nu/V_0) \qquad (14)$$

Here, ν is the number of chains, V_0 is the reference volume obtained during the formation of the network, and I is the coefficient of proportionality. Defined in this manner, κ is proportional to the degree of interpenetration or entanglement of chains in the network. In order to express eq 14 in terms of known and measurable quantities, we use eq 13 and the relationships

$$\nu = \xi/(1 - 2/\phi) \qquad (15)$$

$$\langle r^2\rangle_0^{3/2} = (\langle r^2\rangle_0/M)^{3/2}M_c^{3/2} \qquad (16)$$

$$M_c = (1 - 2/\phi)\rho N_A(\xi/V_0)^{-1} \qquad (17)$$

Substituting these into eq 14 leads to the following relation between κ and v_{2c}:

$$\kappa = A(2C_1)^{-1/2}v_{2c}^{4/3} \qquad (18)$$

with

$$A = I(\langle r^2\rangle_0/M)^{3/2}(1 - 2/\phi)^{1/2}N_A^{3/2}\rho_d^{3/2}(kT)^{1/2} \qquad (19)$$

where N_A is Avogadro's number, and ρ_d is the density of the dry network. For the constrained-junction model A was obtained[6] from various experimental data as $^1/_2$. In the following section we determine the value of A from experimental data on PDMS networks prepared in solution.[9]

Table I
Network Characteristics and Structural Parameters

sample	v_{2C}	$2C_1$	$(\xi kT/V_d)v_{2c}^{2/3}$	κ
B-1	0.879	0.0306	0.0339	5.64
B-2	0.893	0.0337	0.0433	5.17
B-3	0.901	0.0358	0.0499	4.92
B-4	0.914	0.0566	0.0620	4.46
B-5	0.914	0.0583	0.0660	4.33
B-6	0.920	0.0534	0.0695	4.30
B-7	0.927	0.0769	0.0786	4.04
B-8	0.934	0.0893	0.0965	3.72
S1-1	0.669	0.0232	0.0286	3.87
S1-2	0.684	0.0435	0.0493	3.05
S1-3	0.702	0.0593	0.0655	2.76
S1-4	0.698	0.0692	0.0804	2.47
S1-5	0.701	0.0931	0.1058	2.17
S2-1	0.565	0.0272	0.0382	2.52
S2-2	0.577	0.0436	0.0562	2.14
S2-3	0.581	0.0590	0.0670	1.97
S2-4	0.586	0.0799	0.0900	1.73
S2-5	0.583	0.0855	0.0962	1.66
S2-6	0.583	0.0916	0.1059	1.58
S3-1	0.496	0.0295	0.0372	2.03
S3-2	0.547	0.0355	0.0419	2.25
S3-3	0.507	0.0482	0.0552	1.72
S3-4	0.508	0.0517	0.0636	1.62
S3-5	0.514	0.0724	0.0832	1.44
S3-6	0.515	0.0895	0.0933	1.35
S3-7	0.516	0.0992	0.1020	1.30
S4-1	0.465	0.0553	0.0572	1.45
S4-2	0.439	0.0507	0.0665	1.24
S4-3	0.441	0.0655	0.0748	1.16
S4-4	0.449	0.0741	0.0795	1.16
S4-5	0.449	0.0858	0.0821	1.13
S4-6	0.469	0.0920	0.0914	1.16
S4-7	0.469	0.1068	0.0973	1.12
S5-1	0.377	0.0361	0.0406	1.21
S5-2	0.377	0.0449	0.0479	1.11
S5-3	0.382	0.0542	0.0551	1.05
S5-4	0.378	0.0625	0.0589	1.00
S5-5	0.380	0.0689	0.0640	0.96
S5-6	0.381	0.0876	0.0779	0.87
S6-1	0.281	0.0449	0.0389	0.73
S6-2	0.280	0.0390	0.0419	0.71
S6-3	0.280	0.0438	0.0452	0.68
S6-4	0.280	0.0585	0.0566	0.61
S6-5	0.285	0.0841	0.0679	0.56
S6-6	0.282	0.1000	0.0809	0.51

Determination of Parameters from Experimental Data. In the previous comparison of experimental data on PDMS networks cross-linked in solution with the predictions of the constrained-junction model of networks, the κ parameter was found to be related to v_{2c} in the form

$$\kappa = A(2C_1)^{-1/2}v_{2c}^{(4/3)+m} \qquad (18')$$

The coefficient A was determined to be 2, and the values of m ranged from $^2/_3$ and $^8/_9$. In the present study, we use the same data in conjunction with the constrained-chain model to estimate the values of A and m obtained from this model.

The experimental data to be considered had been obtained on 45 samples, which are described in the first three columnes of Table I. The first column gives the sample designation used in the literature,[9] the second the volume fraction of the polymer present in the system during cross-linking, and the third the Mooney–Rivlin estimate of the high-deformation modulus.

The analysis consisted of a global minimization technique applied to the complete set of experimental results available. The procedure is outlined below:

(1) Reasonable initial values are chosen for A and m. Using these values and the experimentally reported values

of $2C_1$ and v_{2c} in eq 18′, a first estimate of κ is adopted for each sample.

(2) The range of the experimental Mooney–Rivlin data considered most reliable was taken to be that in the interval $0.6 < \alpha^{-1} < 0.8$. As in the previous analysis,[6] the strategy is to match theory and experiment at the midpoint of this interval, i.e., at $\alpha^{-1} = 0.7$, and to minimize the differences between theory and experiment at $\alpha^{-1} = 0.6$ and 0.8. Thus, using the value of κ of step 1, we calculate $[f^*]_{\text{ph}}$ from eq 12 to match the published values of $2C_1 + 2C_2/0.7$.[6] We replace the value of $2C_1$ in eq 18′ with this value of $[f^*]_{\text{ph}}$ and obtain a new κ. We iterate these steps until the calculated values of κ converge.

(3) Using the values of $[f^*]_{\text{ph}}$ and the κ obtained in the previous step, we obtain $[f^*]$ from eq 12 for $\alpha^{-1} = 0.6$ and 0.8.

(4) The error for this choice of A and m is calculated from

$$\text{error} = \sum_{i=1}^{45}\{([f^*]_{\alpha^{-1}=0.6} - 2C_1 - 2C_2/0.6)_i^{\,2} + ([f^*]_{\alpha^{-1}=0.8} - 2C_1 - 2C_2/0.8)_i^{\,2}\}/45$$

where the subscript i indicates that the quantities within the parentheses are calculated for the ith sample.

(5) The value of m is changed, and the corresponding change in the value of κ is recalculated from eq 18′. The value of $[f^*]_{\text{ph}}$ matching the experimental value of $2C_1 + 2C_2/0.7$ is recalculated from eq 12 with this new value of κ, and steps 3 and 4 are repeated until the value of m giving the smallest error is obtained.

(6) The value of A is changed, and the corresponding change in the value of κ is recalculated from eq 18′. The value of $[f^*]_{\text{ph}}$ matching the experimental value of $2C_1 + 2C_2/0.7$ is recalculated from eq 12 with this new value of κ, and steps 3–5 are repeated until the error reaches a minimum.

Results and Discussion

The minimum error thus obtained was found for $A = 1.29$ and $m = 0.385$. The corresponding values of the front factor $(\xi kT/V_d)v_{2c}^{2/3}$ and of κ for each of the samples are given in the last two columns of Table I. The values of κ obtained from the constrained-chain model are significantly smaller, by about 40%, than those obtained from the constrained-junction model. This was to be expected since the constraints are now imposed along the entire chain contours, instead of being arbitrarily concentrated only on the junctions. It is most encouraging to compare this result with very recent neutron scattering results from labeled junctions in networks.[10] The measured junction fluctuations were found to be considerably larger than expected by applying the constrained-junction theory to the corresponding stress–strain isotherms. This is consistent with the constraints being spread out from the junctions, onto the chains themselves, as is implied by the lower values of κ.

Isotherms were then calculated for all the samples using the obtained values of A and m in eq 12. The results for three typical samples, S-1, S1-5, and B-4, are compared with the experimental data points in Figure 2. There is seen to be very good agreement.

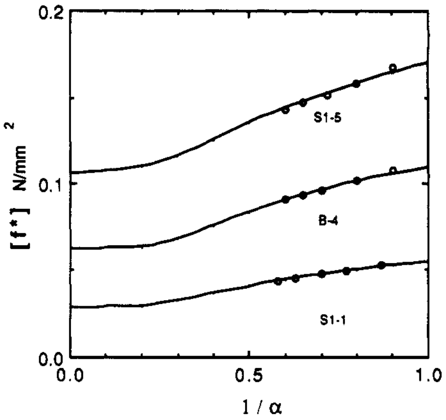

Figure 2. Illustrative stress–strain isotherms in the Mooney–Rivlin representation. The circles locate the experimental points,[9] and the curves have been calculated from the constrained-chain theory.

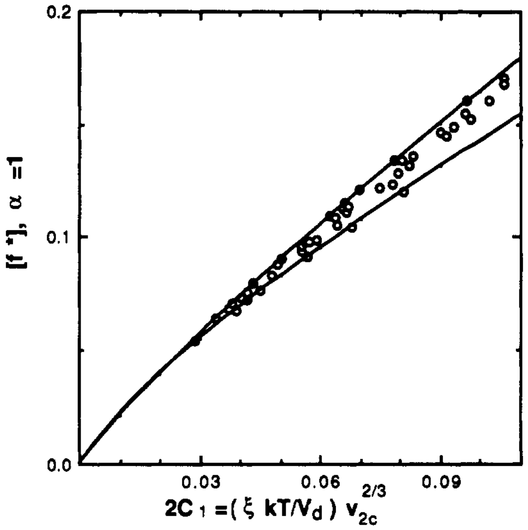

Figure 3. Low-deformation modulus shown as a function of the Mooney–Rivlin $2C_1$ constant and the front factor it approximates. The experimental data points are well described by the two curves calculated from the constrained-chain theory.

Figure 3 presents values of the low-deformation modulus as a function of the front factor $(\xi kT/V_d)v_{2c}^{2/3}$. The two lines have been calculated from the constrained-chain theory, eq 18′, using the parameters obtained as described above. The lower line was calculated for $v_{2c} = 0.28$, the minimum value of this variable, and the upper line for $v_{2c} = 0.90$, the maximum value. All the experimental points fall within the region demarcated by the two limiting values of v_{2c}. This is important because the relationship between the moduli at small deformations and the cross-link density has been the subject of major disagreement among various workers primarily because of the belief that entanglement contributions should be greatest at small deformations. The data on the dried samples at $\alpha = 1$ compare favorably with the predictions of the constrained-chain model, however, and additional trapped-entanglement contributions do not seem to be necessary. This may be due to relatively low chain entangling in PDMS, as suggested by its value of the plateau modulus, and it would therefore be quite important to carry out analogous experiments on neworks prepared using polymer chains exhibiting a significantly larger plateau modulus.

Such additional experiments would also be useful for determining whether the values of A and m obtained in the present investigation are universal and therefore useful for interpreting and even predicting the elastomeric properties of a variety of rubberlike materials. It should be pointed out, however, that while the proportionality constant A is well-defined, the newly introduced parameter m is not yet well-defined and much further work is required to interpret its physical meaning.

Acknowledgment. It is a pleasure to acknowledge financial support provided by the National Science Foundation through Grant DMR 89-18002 (Polymers Program, Division of Materials Research) and the Research Fund of Bogazici University, Grant No. 91P0029.

References and Notes

(1) Flory, P. J. *Proc. R. Soc. London, A* **1976**, *351*, 351.
(2) Edwards, S. E.; Vilgis, T. A. *Rep. Prog. Phys.* **1988**, *51*, 243–297.
(3) Flory, P. J. *J. Phys. Chem.* **1977**, *66*, 5720.
(4) Ronca, G.; Allegra, G. *J. Chem. Phys.* **1975**, *63*, 4990.
(5) Erman, B.; Monnerie, L. *Macromolecules* **1989**, *22*, 3342.
(6) Erman, B.; Mark, J. E. *Macromolecules* **1987**, *20*, 2892.
(7) Mark, J. E.; Erman, B. *Rubberlike Elasticity: A Molecular Primer*; Wiley-Interscience: New York, 1988; p 196.
(8) Erman, B.; Flory, P. J. *Macromolecules* **1982**, *15*, 806.
(9) Johnson, R. M.; Mark, J. E. *Macromolecules* **1972**, *5*, 41.
(10) Ewen, B. In *Elastomeric Polymer Networks*; Mark, J. E., Erman, B., Eds.; Prentice-Hall: Englewood Cliffs, NJ, 1992.